SEISMIC RISK AND THE DENALI FAULT

Part II.
Seismic Response Analyses and Simulated Earthquake Motion

H. Pulpan
R. B. Forbes

Prepared for Gulf Interstate Engineering Company

Geophysical Institute
University of Alaska
Fairbanks, Alaska 99701

April, 1977

ABSTRACT

Seismic Risk and the Denali Fault, Part II, presents the results of seismic response analyses of four additional sections, taken from deep water well logs from important localities along the Delta Junction-Alaska-Canada Boundary segment of the proposed Alcan gas pipeline route. These models were added to the study, based on the need for additional data on the response of thicker sections of surficial materials, with water tables of varying depth and the effect of shallow permafrost.

The initial seismic response analyses were based on input motion from the magnitude 7.7 Kern County earthquake of 1952, as recorded at Pasadena, modified to better represent the motion expected from a magnitude 8 earthquake on the Denali Fault.

Due to uncertainties in the use of scaling factors in the higher magnitude ranges, we decided to submit the model sections to a simulated earthquake which more closely matched the motion which would be generated by strain release on the Denali Fault, 50 km from the site.

Response to the two types of input motion was quite similar with respect to the maximum acceleration values developed at the surface. However, the artificial earthquake produced an increased number of strain cycles, which would be important in the case of liquefiable soils. The results of both studies indicate that calculated maximum accelerations in surface materials are unlikely to exceed 0.50 g and that design criteria along most of the route segment will be similar to those developed for other high seismic risk zones. The liquefaction problem deserves further study; but such studies should not be attempted without more detailed sampling and adequate soils engineering data.

TABLE OF CONTENTS

INTRODUCTION

In our initial report, *Seismic Risk and the Denali Fault, Part I,* we presented data derived from seismic response analyses of representative subsurface sections along the Delta Junction-Alaska-Canada boundary segment of the proposed Alcan gas pipeline route.

In the previous study, the sections were subjected to the motion recorded at Pasadena during the 1952 Kern County earthquake. In this report, we present results which were obtained when the same sections were submitted to a design earthquake which we believe more closely simulates the motion which would be associated with a strain release generated by a magnitude 8 earthquake along the Denali Fault.

This report also includes seismic response analyses of additional sections with increased total thickness and known water tables. These sections are taken from selected water well logs obtained from State of Alaska and U.S. Corps of Engineers hydrologic records.

SEISMIC RESPONSE ANALYSIS

Analyses of Additional Sections

Four additional surficial sections were subjected to seismic response analysis, using the techniques outlined in Part I. These sections, which were taken from water well logs (Waller and Tollen, 1962a, 1962b), are shown in Figure 1. Some of these sections are substantially thicker than those analyzed in Part I, but otherwise consist of similar types of materials. For convenience, the profiles analyzed in Part I of this report are reproduced in Figure 2.

In the absence of new drilling and laboratory data for these profiles, we have used the engineering parameters derived from the test hole data used in Part I. The soil properties of the new section MOD are comparable to those of section A6-9, while the remaining new sections are similar to section A2-11. The input motion used in the analysis of the new profiles was again the Pasadena motion of the magnitude 7.7, 1952 Kern County earthquake, scaled to a maximum acceleration of 0.2 g and a predominant period of 0.4 seconds. Additionally, both the new profiles and those analyzed in Part I have been subjected to a simulated earthquake, as discussed below.

Generation of Simulated Earthquake Motion

In Part I, we discussed the multitude of empirical relationships, which have been derived for strong ground motion, and the large scatter in the actual measurements. The lack of adequate data, especially in the magnitude 8 range, was also discussed. This situation along with an inadequate understanding of the mechanics of generation and propagation of strong motion to surface locations, have led investigators to the generation of simulated earthquake accelerograms, based on statistical considerations. Models of varying complexity have been used, including White Noise, stationary Gaussian processes and non-stationary processes of various types.

We have subjected the selected sections to such artificially generated ground motion, following the approach of Jennings et al. (1968) and Ruiz and Penzien (1969). Essentially, a Gaussian White Noise generated on the computer through a random number-generating routine is passed through a filter to provide the proper frequency content. A shaping window is then applied to give the simulated motion the initial build-up and exponential decay typical of actual recordings. The filter parameters and shaping function, as well as the duration and expected maximum acceleration, were chosen to generate a simulated earthquake with the basic characteristics presented in Part I for a magnitude 8 earthquake on the Denali Fault.

Figures 3 and 4 show the time histories and Fourier amplitude spectra of the Pasadena and artificial earthquake, respectively. The most obvious difference between the two motions is a more rapid build-up in the artificial earthquake toward the high intensity portion of the motion. The Pasadena motion was recorded about 100 km from the epicenter. The difference in arrival time of the P and S phases, respectively, would be about 13 seconds. If the horizontal component is triggered by a P wave converted into a S wave at some discontinuity, the P-S difference will be somewhat shortened. The Pasadena earthquake record probably reflects such a situation. The artificial earthquake has been recorded at 50 km from the epicenter. Though the build-up is somewhat rapid in the artificial record, it is probably a good simulation of what would occur in the strong motion record of our design earthquake.

The spectra of the two motions are quite similar, with the exception of longer amplitudes in the frequency band below one cycle per second in the artificial earthquake. We expected less high frequency content in the Pasadena motion, as compared to the artificial earthquake. Due to the difference in epicentral distances, the high frequency waves attenuate more rapidly with distance than low frequency waves, but this effect is not reflected in the spectra.

Clearly, the use of simulated earthquake motion will not overcome our ignorance about the complex wave mechanics involved in the explanation of a seismic record as generated by a particular earthquake, but it does enable us to generate simulated records which may more closely approach the parameters of a design earthquake for a given situation.

Discussion

Figures 5 through 8 show the time history of surface acceleration, the Fourier amplitude spectrum of that motion, the soil transfer function, and the time history of the shear strain in the middle of the top layer for four sections.

In these figures the input is the Pasadena motion. Figures 9 through 12 show for the same sections the same quantities, but the input motion is the simulated earthquake record. From Figures 3 and 4 and plots 1 through 5, it is apparent that there is little difference in the response to the two motions. For a given section, the maximum surface accelerations are very similar. The main difference is again seen in the more rapid rise towards the high intensity motion in the artificial earthquake. Comparing the strain records for a given profile resulting from the two motions, there is an increased number of significant strain cycles in the artificial record. This would be important in the case of liquefiable soils, as the number of significant stress cycles is a decisive parameter in determining whether a vulnerable soil will approach liquefaction.

The additional sections have been subjected to both motions. The results shown in Tables 3 and 4, if compared to the data in Part I, Tables 1 and 2, reinforce our conclusions that an increase in the thickness of the section would reduce the peak acceleration values at the surface, since the peaks of the soil transfer functions occur in a frequency band where the input motion contains less power. The shift in the transfer function peaks towards lower frequencies with increasing depth can be seen in the figures. Note that the transfer functions shown in the figures refer to the ratio of acceleration (as a function of frequency) that would be developed on the top soil layer, over the acceleration that would occur in bedrock outcrops. In calculating these transfer functions, the strain dependence of the soil parameters is not taken into account; hence they are independent of the actual input motion. The spectral amplifications given in Tables 1 and 2, however, refer to the ratios between the acceleration at the surface and those at the interface between bedrock and the bottom soil layer. Since the acceleration will always be greater for outcrops as compared to buried bedrock, the peak values given in the tables for each section show higher values than corresponding peak values in the plots of the transfer functions.

CONCLUSIONS AND RECOMMENDATIONS

A one-dimensional shear wave propagation model has been used to analyze the response of several surficial sections along the Delta Junction-Alaskan Canada Boundary segment of the proposed Alcan gas pipeline route to strong motion associated with a magnitude 8 earthquake generated by the Denali Fault. ,45 The analyses concentrate on sections incorporating surficial materials and conditions which might require special design considerations, from the standpoint of seismic risk.

Although the analyses suffer from the lack of precise soils engineering data, which negates the application of more sophisticated analysis, we can offer the following conclusions:

1. Maximum surface accelerations developed along the proposed pipeline between Delta Junction and the USA-Canada boundary will not require any special design consideration beyond those routinely required in high seismic risk zones.

2. Test hole data indicate that low-cohesion, water saturated soils may occur at a few localities along this point of the route. These soils would liquefy under the motion produced by our design earthquake. Therefore, we recommend the following studies:

(a) Delineation of areas with potentially liquefiable soils, with special attention to river crossings and south-facing loess-covered hills.

(b) Acquisition of adequate engineering parameters for representative and critical soil types.

(c) Re-evaluation of the liquefaction potential, on the basis of the data obtained from (a) and (b) above.

(d) Calculation of acceleration, velocity, and displacement response spectra from analyses based on the improved data.

(e) Development of design spectra for varying surficial conditions.

REFERENCES

Jennings, P. C., G. W. Housner, and N. C. Tsai, 1968, Similulated earthquake motions: EERL Cal. Tech. Report, 22 pp.

Ruiz, P., and J. Penzien, 1969, Artificial generation of earthquake accelerograms: EERC, Univ. of Calif., Berkeley, NISEE Computer Applications.

Waller, Roger M., and Donald A. Tolen, 1962a, Data on wells along the Alaska Highway (State 2), Alaska: U.S. Geol. Survey, Report No. 18, 26 pp.

Waller, Roger M., and Donald A. Tolen, 1962b, Data on wells and springs along the Richardson Highway (State 4), Alaska: U.S. Geol. Survey, Report No. 16, 32 pp.

Table 1. Maximum surface accelerations (in g) developed in different profiles due to Pasadena motion scaled to 0.1 g maximum accelerations. (A6-7a is A6-7 profile with permafrost removed).

Profiles	A3-2	A6-7	A6-7A	A6-9	A2-7	A2-11
Depth to bedrock 60 ft (except in A3-2, 8 ft)	.11	.17	.17	.22	.19	.24
Depth to bedrock 200 ft (except in A3-2, 60 ft)	.24	.13	.14	.11	.18	.19

Table 2. Maximum surface accelerations (in g) developed in different profiles due to Pasadena motion scaled to 0.2 g maximum accelerations. (A6-7a is A6-7 profile with permafrost layer removed.

	A3-2	A6-7	A6-7A	A6-9	A2-7	A2-11
Depth to bedrock 60 ft (except in A3-2, 8 ft)	.22	.24	.25	.39	.41	.44
Depth to bedrock 200 ft (except in A3-2, 60 ft)	.41	.20	.21	.21	.34	.36

Table 3. Maximum surface acceleration (in g) developed in different prifiles due to different input motions (DEL = Delta Junction profile; TOK = Tok Junction profile; CHEM = Chemical Test Site profile; MOD = Sand Model).

Profiles	DEL	TOK	CHEM	MOD
Modified Pasadena motion (.2 g max. accel.)	.13	.24	.14	.25
Artificially-generated record (.2 g max. accel.)	.10	.21	.13	.27

Table 4. Maximum surface acceleration (in g) developed in different profiles due to artificially-generated record with 0.2 g maximum acceleration. (A6-7A is A6-7 profile with permafrost layer removed.)

Profiles	A3-2	A6-7	A6-7A	A6-9	A2-7	A2-11
Depth to bedrock 60 ft (except in A3-2, 8 ft)	.30	.26	.27	.33	.43	.47
Depth to bedrock 200 ft (except in A3-2, 60 ft)	.37	.20	.20	.19	.30	.31

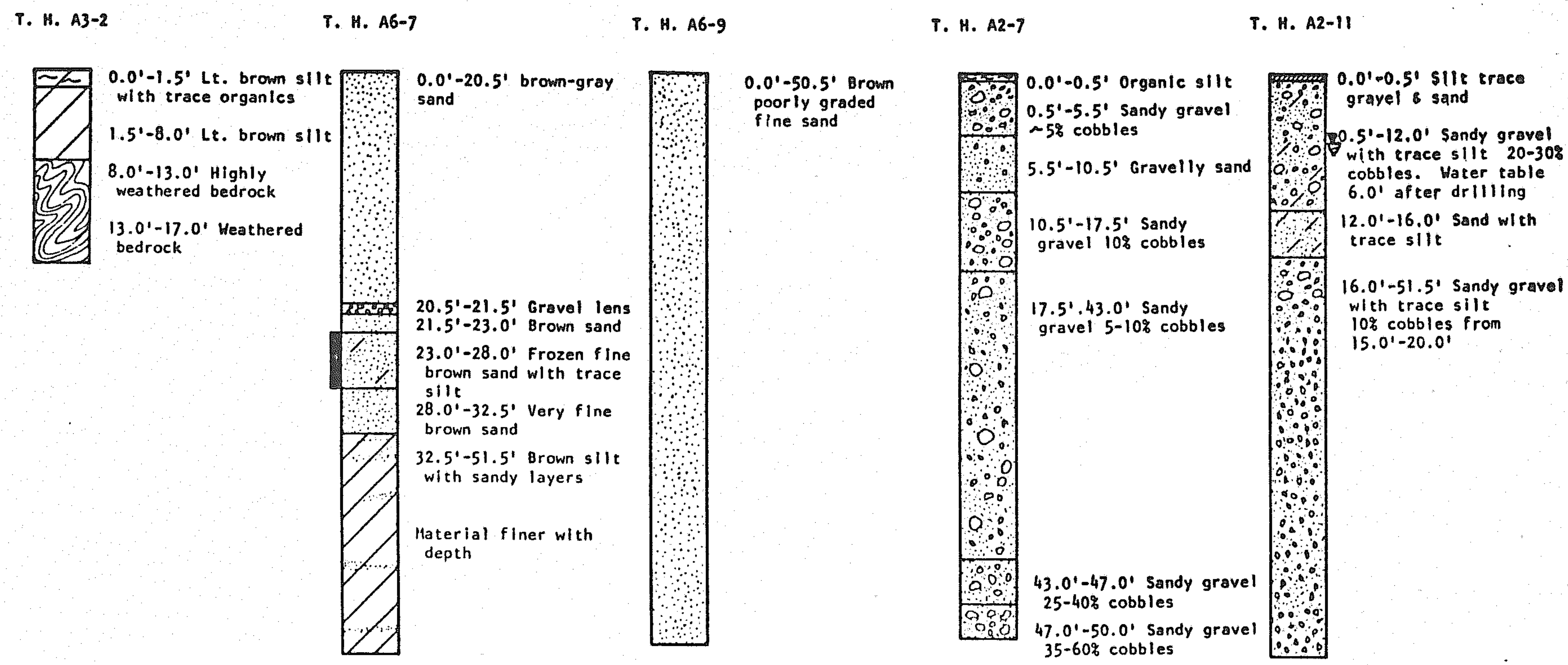

Figure 1. Stratigraphic sections used for seismic response analysis (Part I).

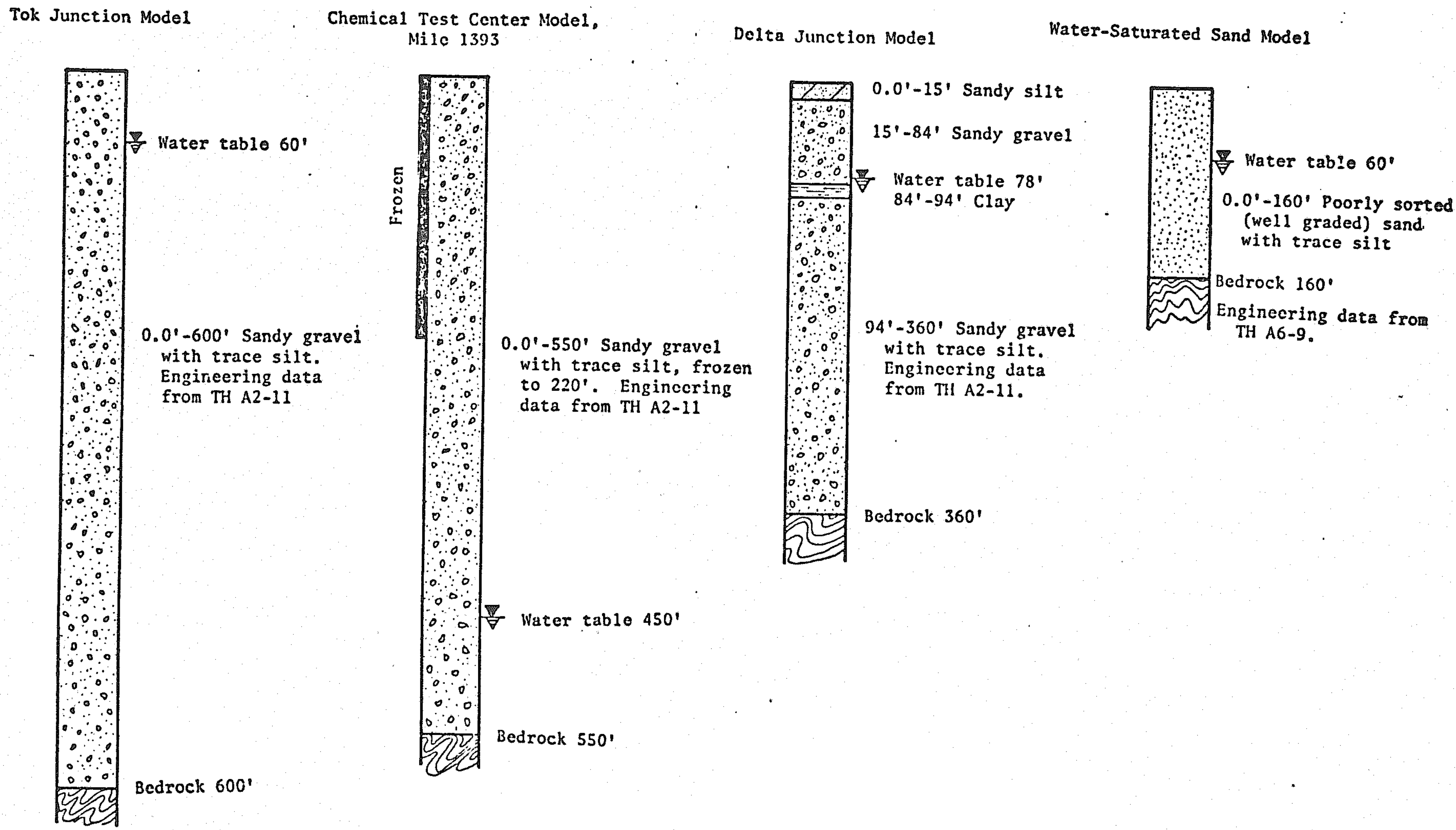

Figure 2. Sections used in seismic response analysis.

FIGURE 3. TIME HISTORY (LEFT) AND FOURIER AMPLITUDE SPECTRUM (RIGHT) OF MODIFIED PASADENA MOTION (MAGNITUDE 7.7, 1952 KERN COUNTY EARTHQUAKE) USED IN THE ANALYSIS.

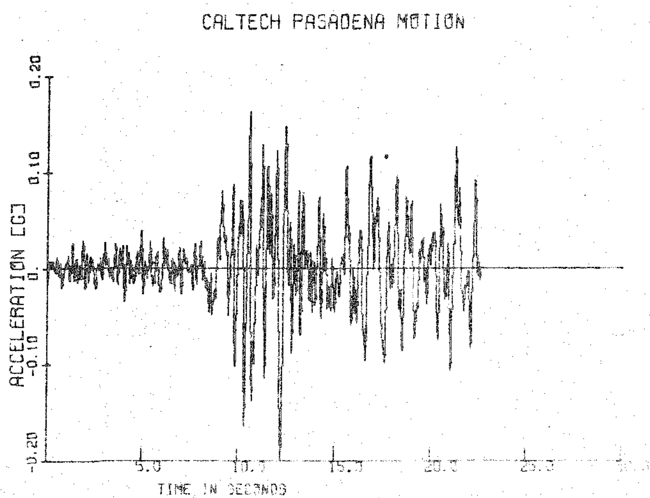

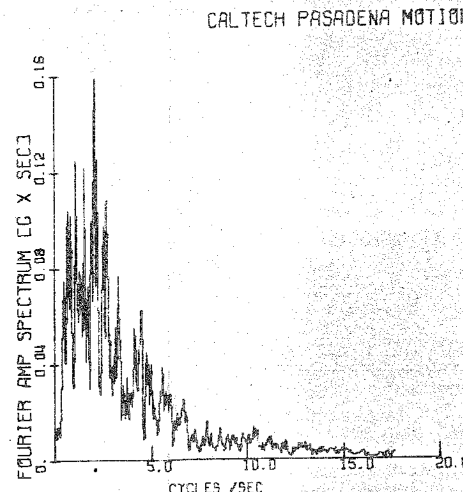

FIGURE 4. TIME HISTORY (LEFT) AND FOURIER AMPLITUDE SPECTRUM (RIGHT) OF ARTIFICIALLY GENERATED RECORD USED IN THE ANALYSIS.

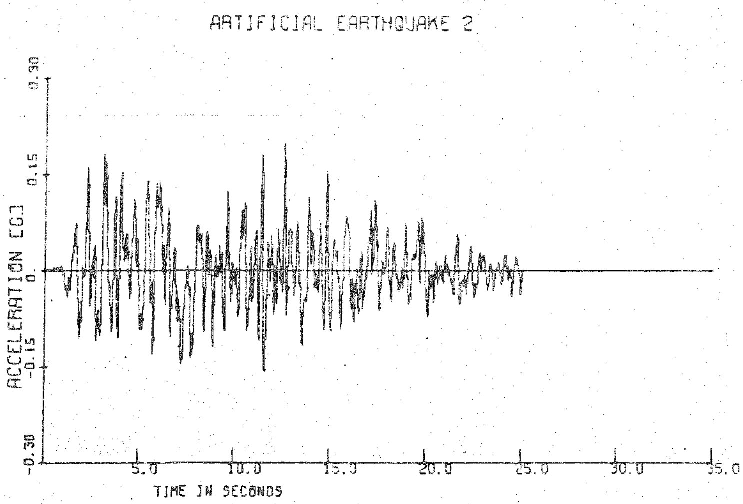

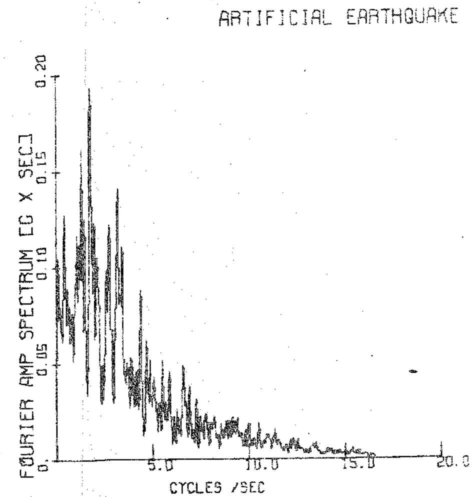

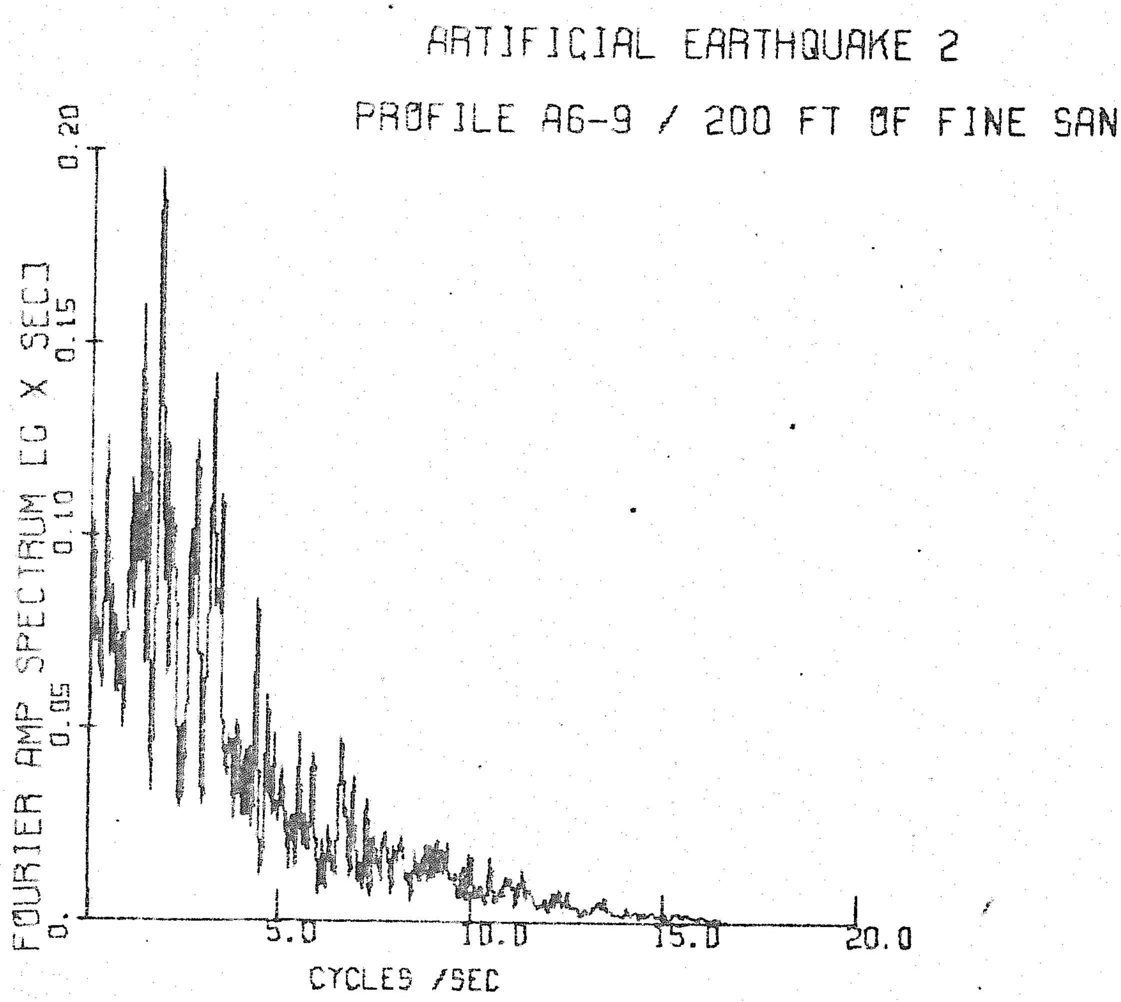

FOURIER AMPLITUDE SPECTRUM OF SURFACE MOTION

FIGURE 5. SOIL PROFILE A3-2 (8 FT. TO BEDROCK)
PASADENA RECORD

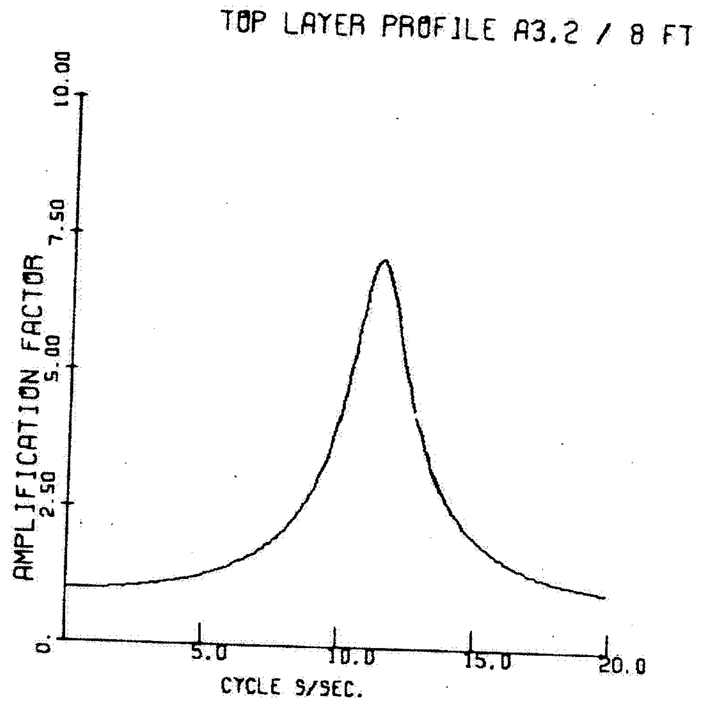

Soil Transfer Function

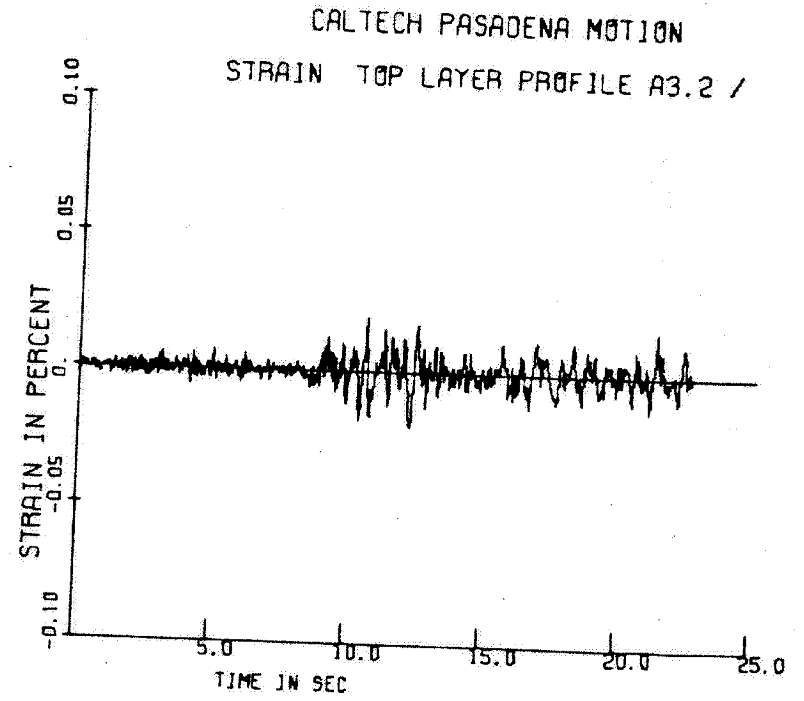

Time History of Strain on Top Soil Layer

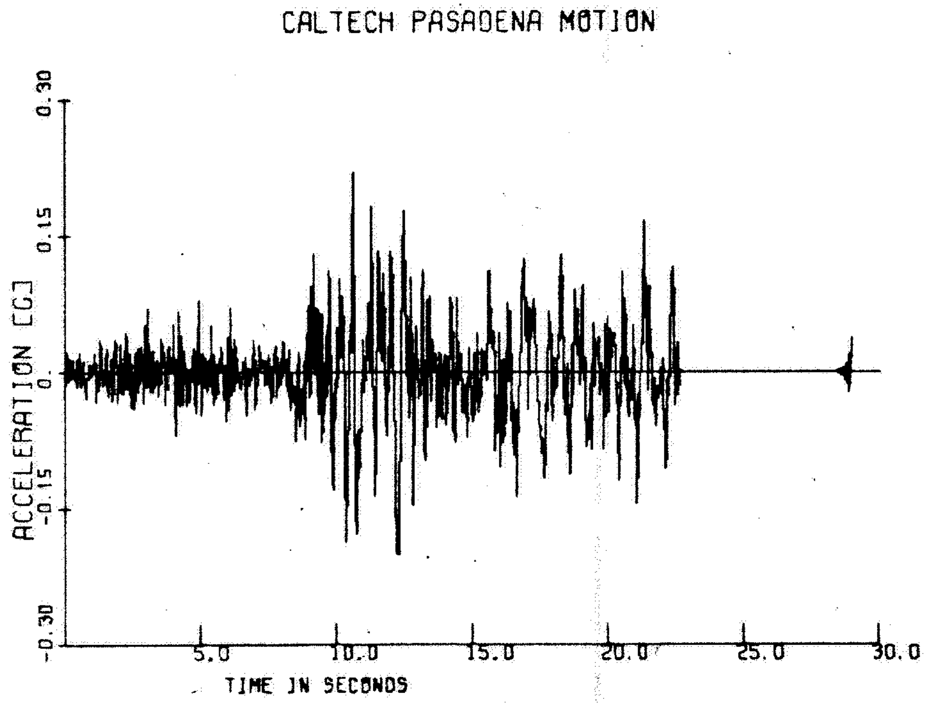

Time History of Surface Acceleration

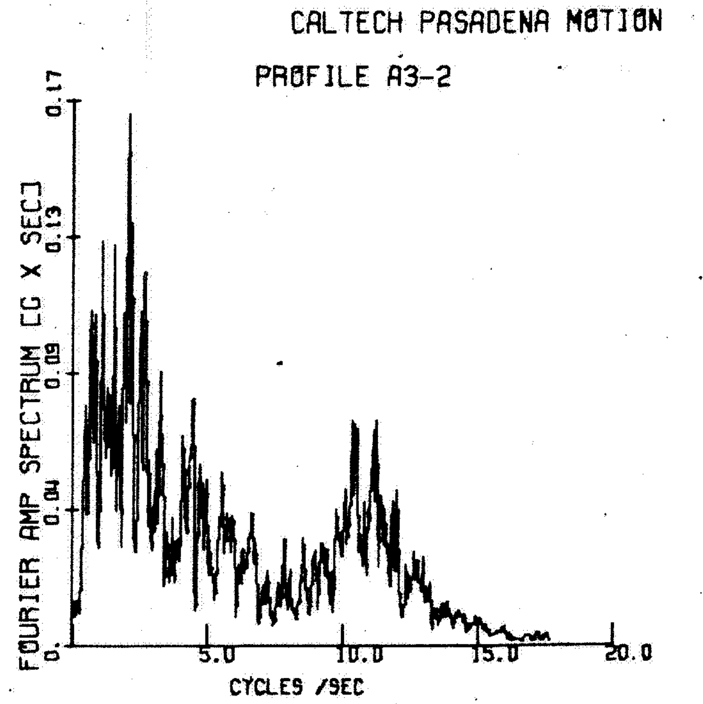

Fourier Amplitude Spectrum of Surface Motion

FIGURE 6. SOIL PROFILE A2-11 (60 FT. TO BEDROCK)
PASADENA RECORD.

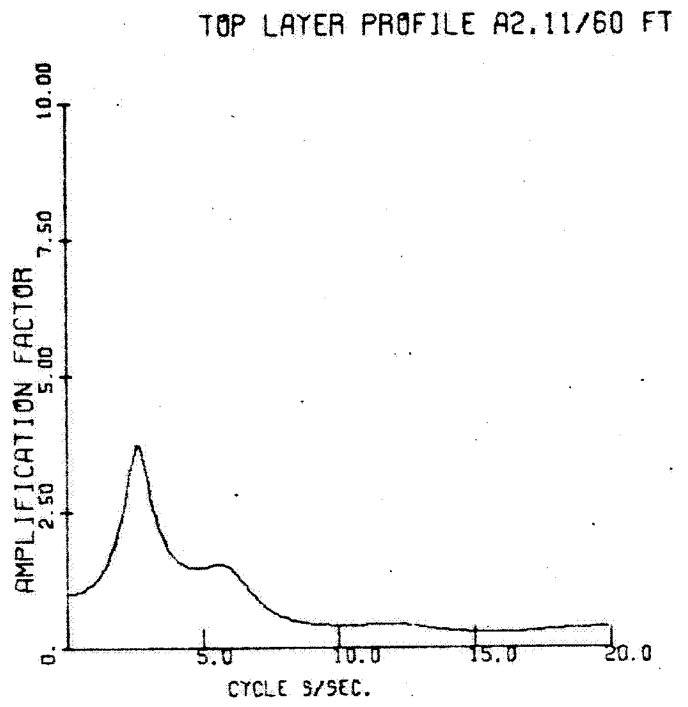

Soil Transfer Function

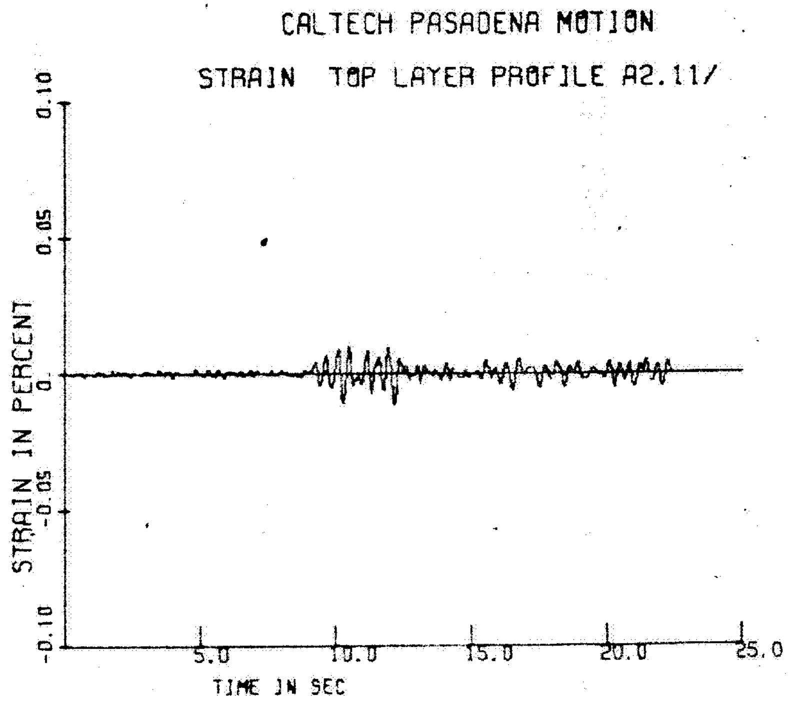

Time History of Strain on Top Soil Layer

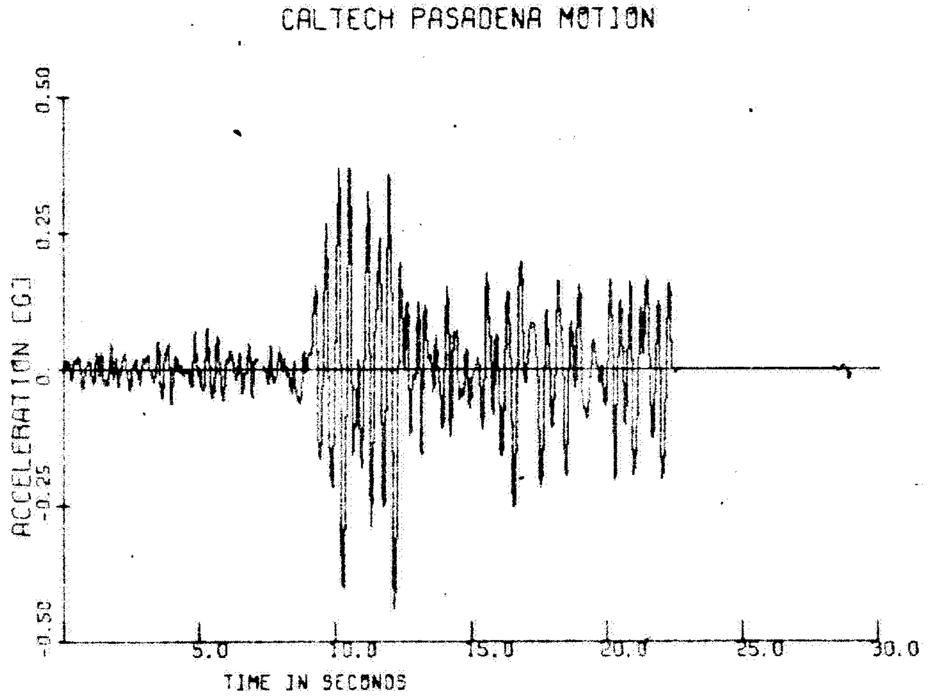

Time History of Surface Acceleration

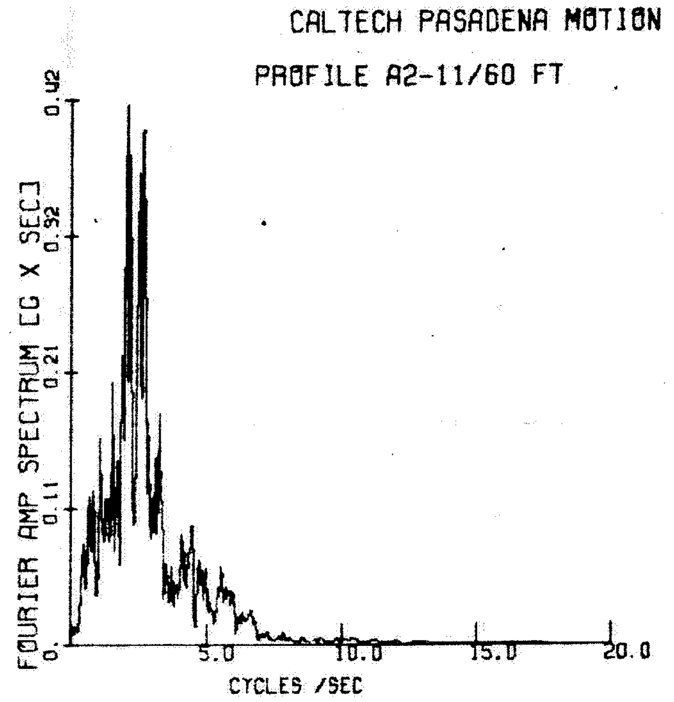

Fourier Amplitude Spectrum of Surface Motion

FIGURE 7. SOIL PROFILE A6-9 (60 FT. TO BEDROCK)
PASADENA RECORD

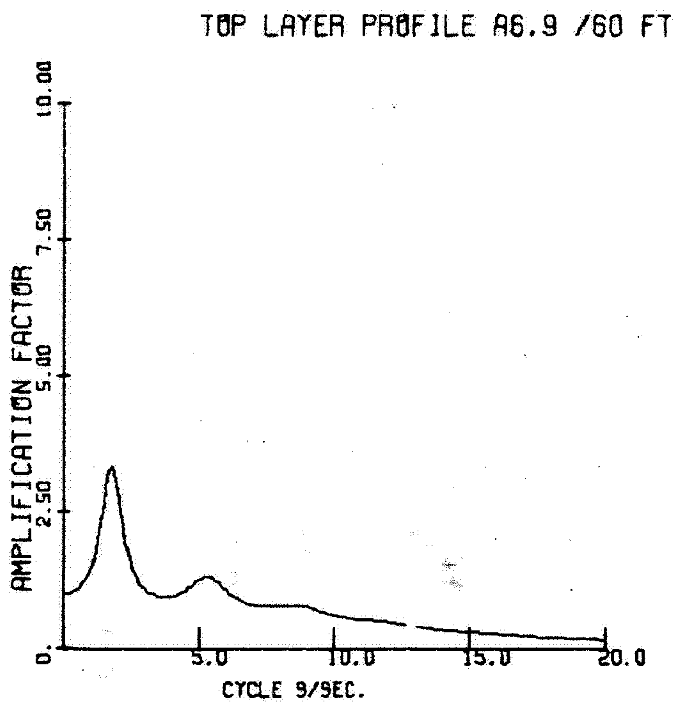

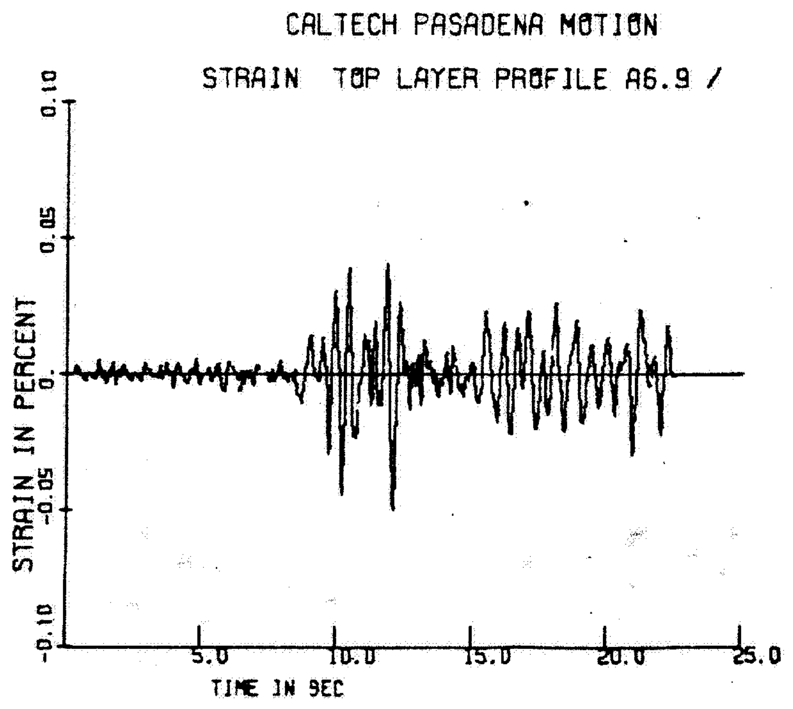

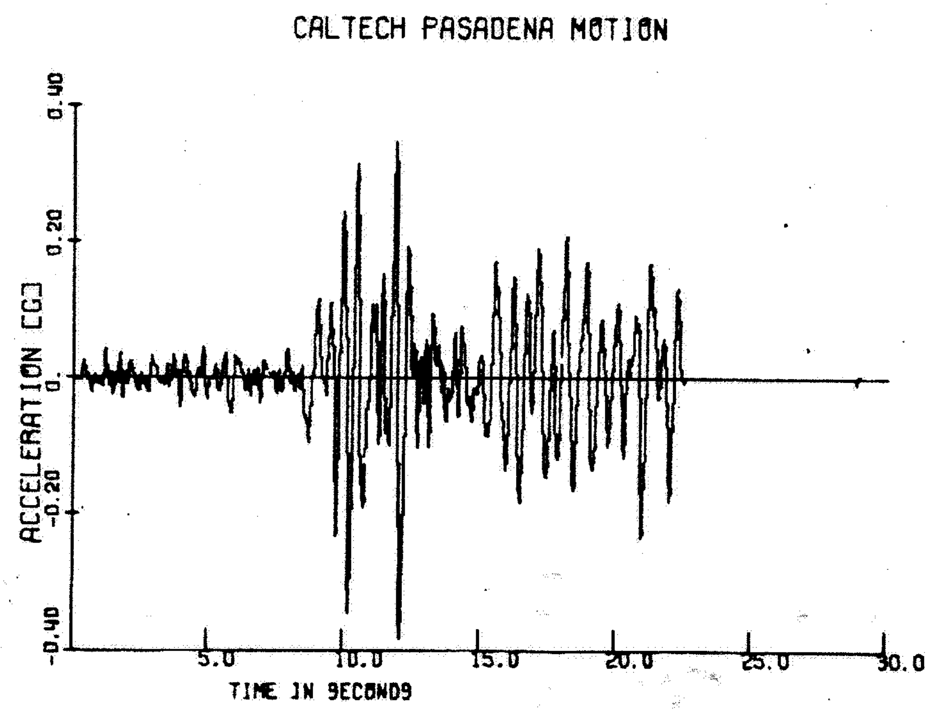

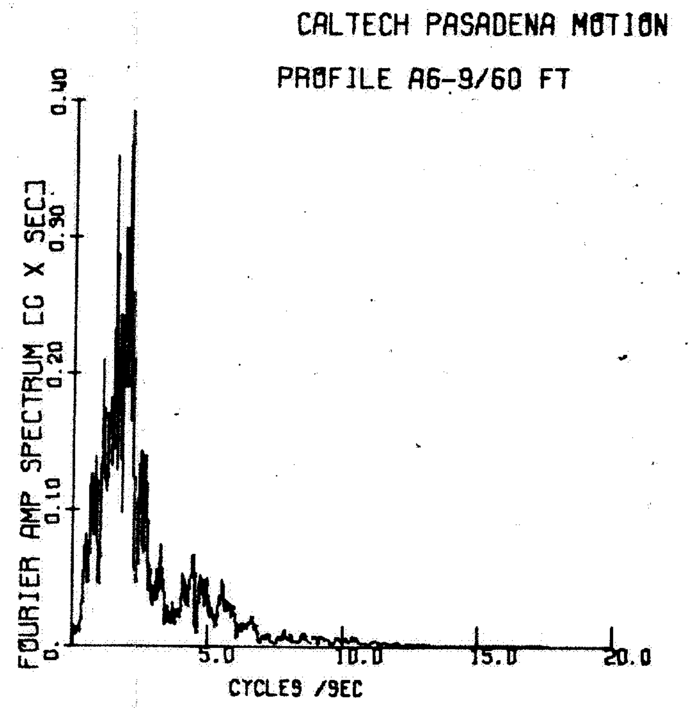

Fourier Amplitude Spectrum of Surface Motion

FIGURE 8. SOIL PROFILE A6-9 (200 FT. TO BEDROCK)
PASADENA RECORD

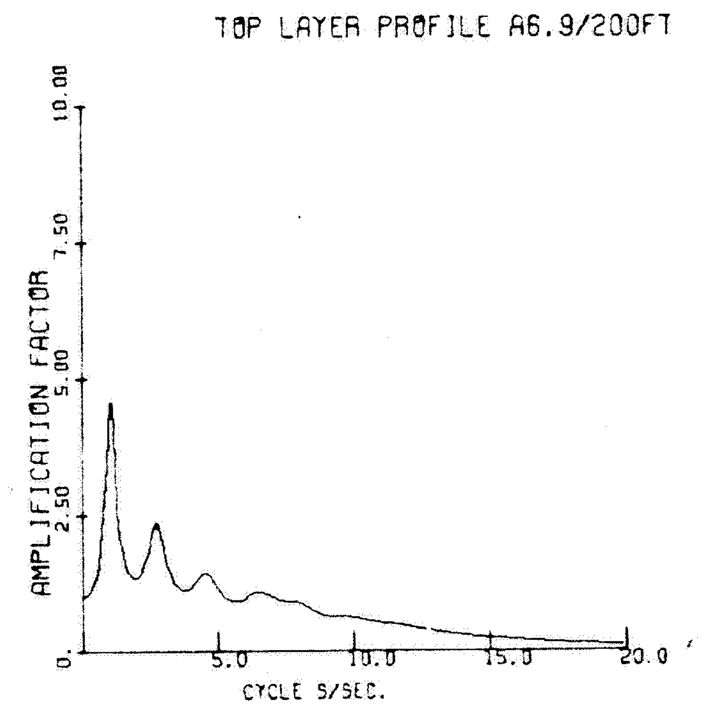

Soil Transfer Function

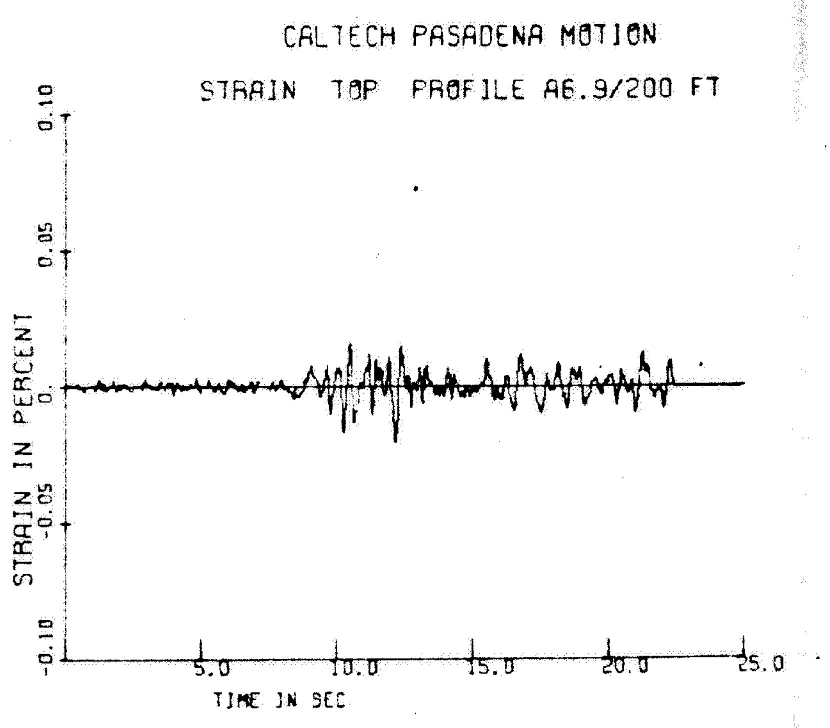

Time History of Strain on Top Soil Layer

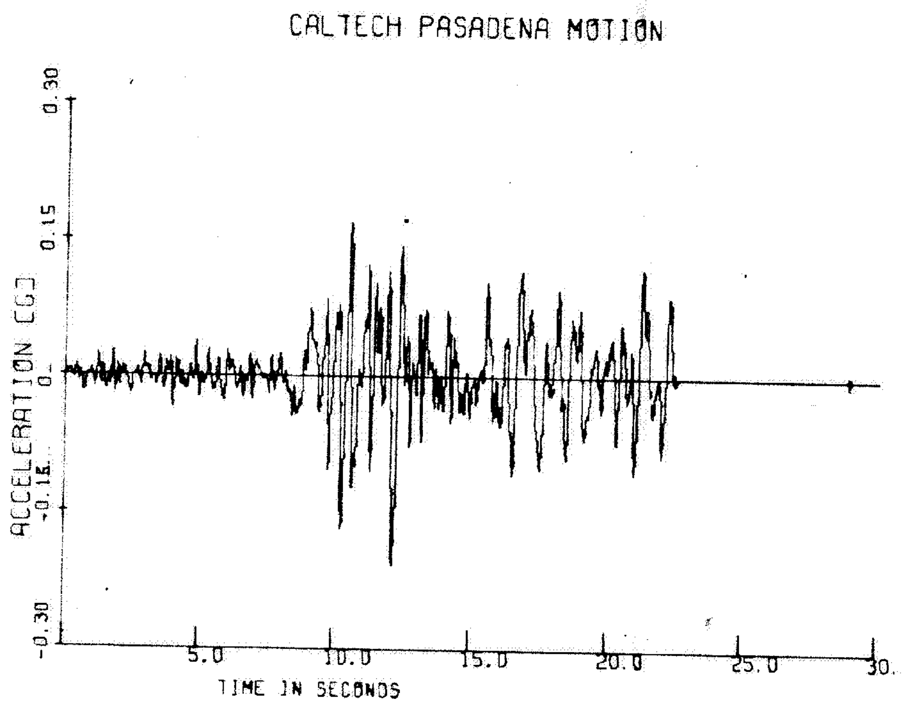

Time History of Surface Acceleration

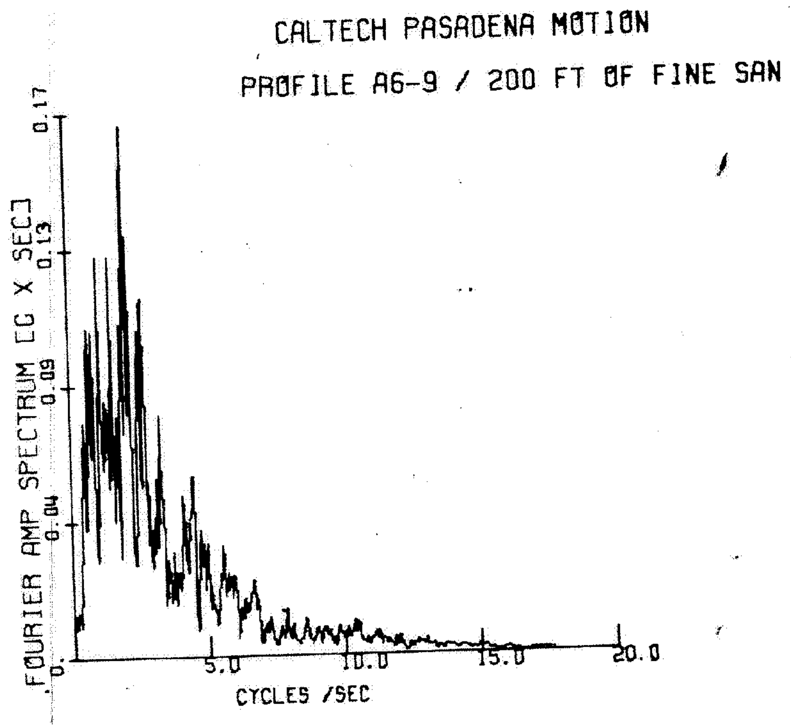

Fourier Amplitude Spectrum of Surface Motion

FIGURE 9. SOIL PROFILE A3-2 (8 FT. TO BEDROCK)
SIMULATED EARTHQUAKE

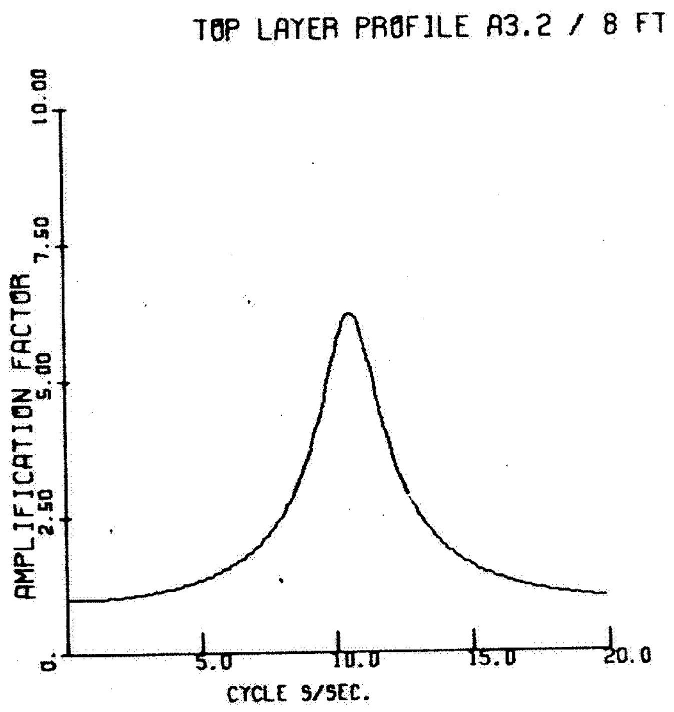

Soil Transfer Function

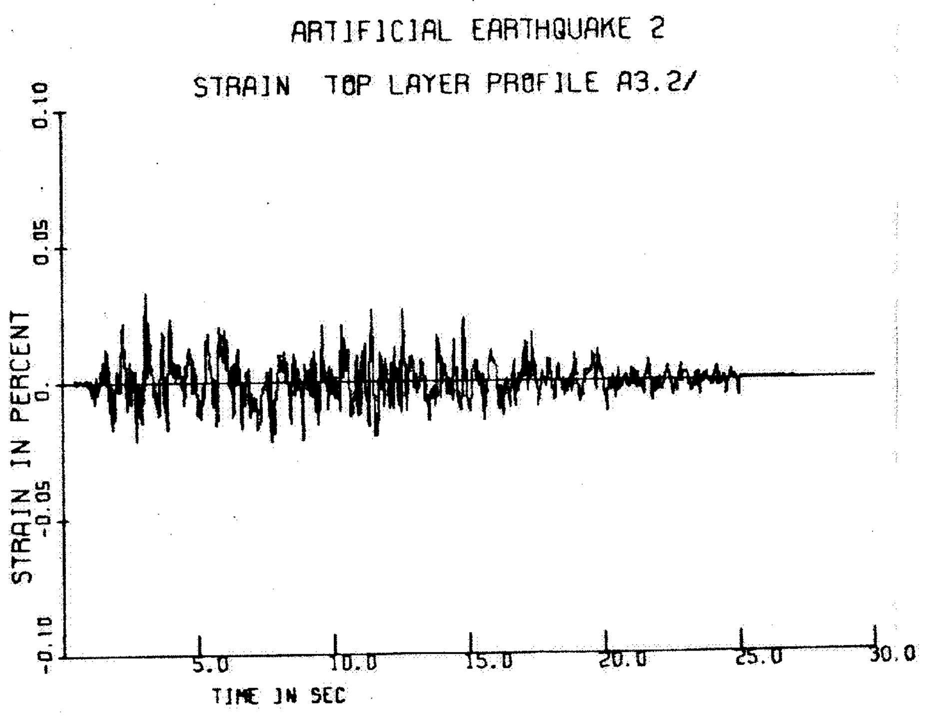

Time History of Strain on Top Soil Layer

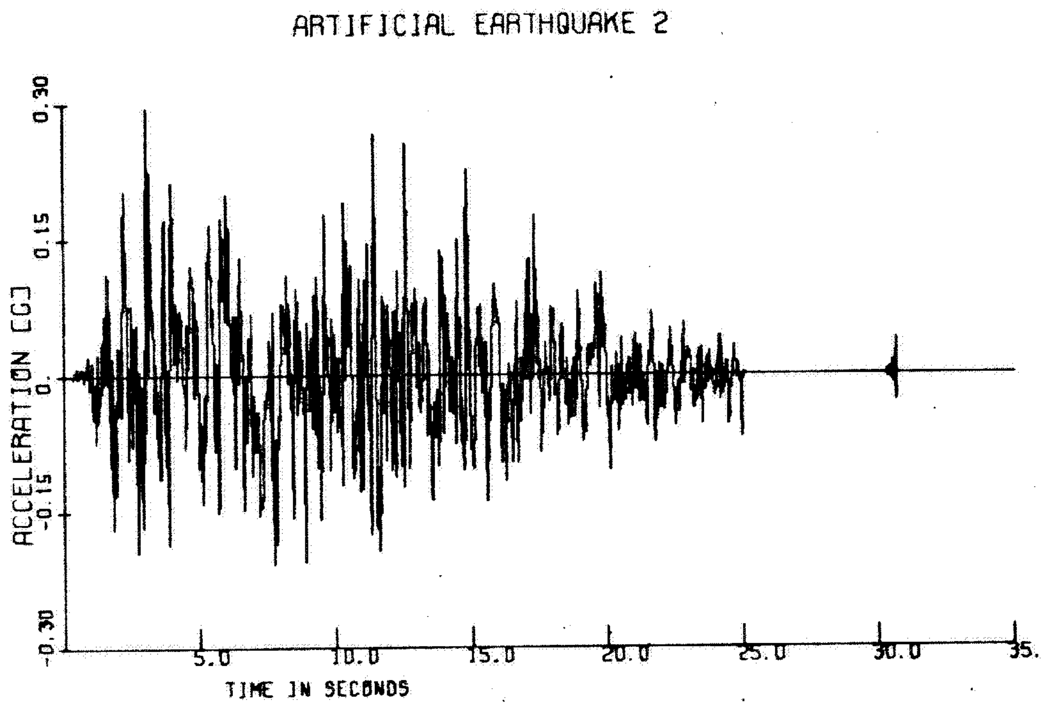

Time History of Surface Acceleration

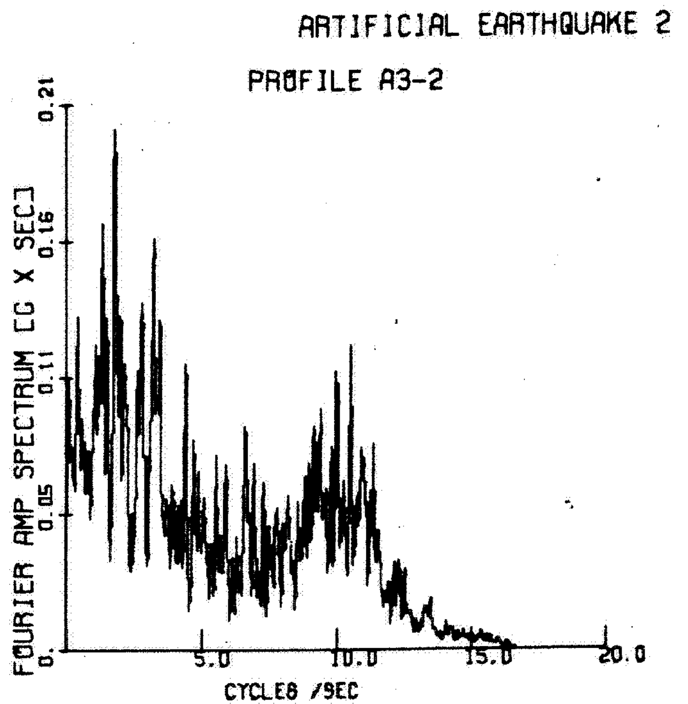

Fourier Amplitude Spectrum of Surface Motion

FIGURE 10. SOIL PROFILE A2-11 (60 FT. TO BEDROCK)
SIMULATED EARTHQUAKE

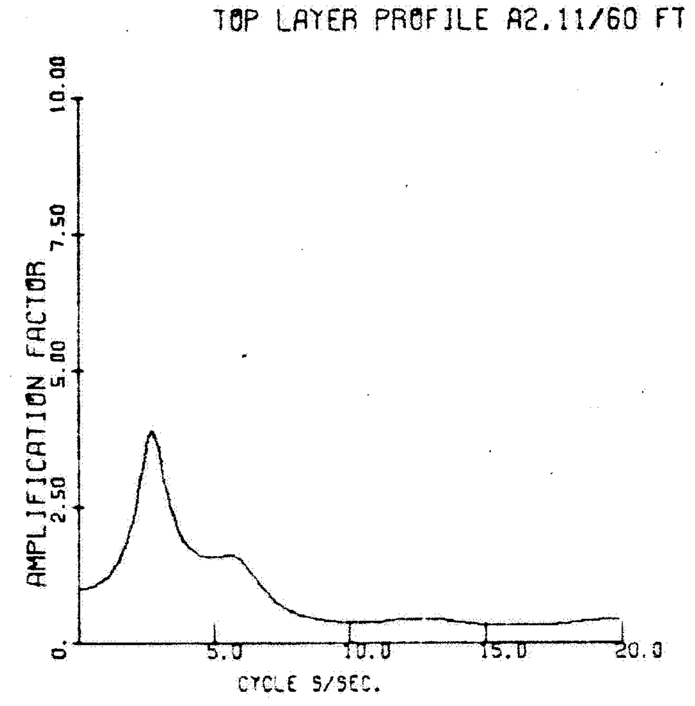

Soil Transfer Function

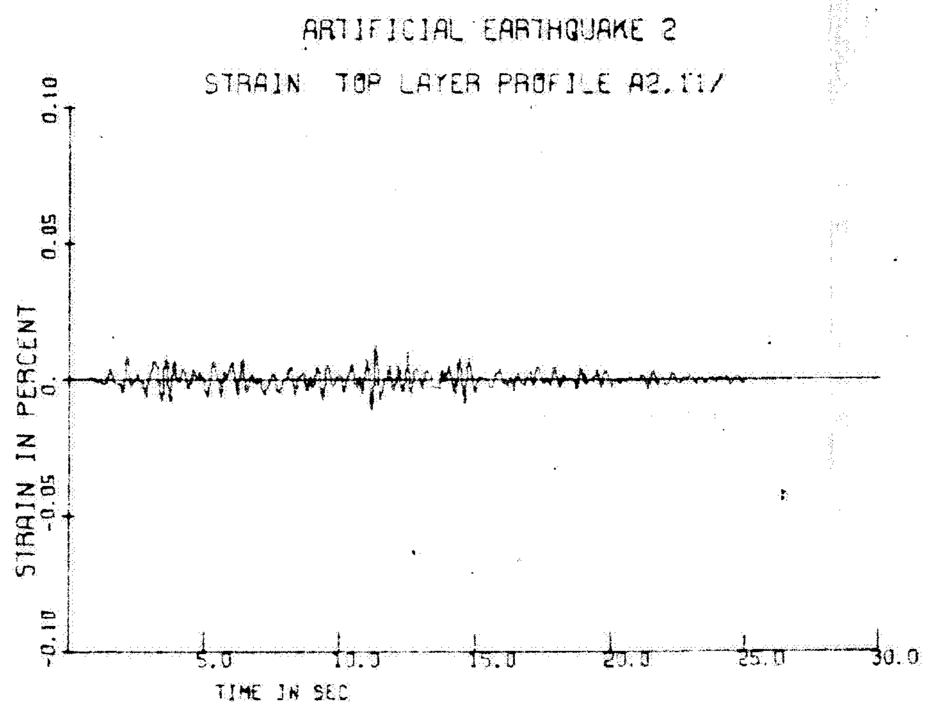

Time History of Strain on Top Soil Layer

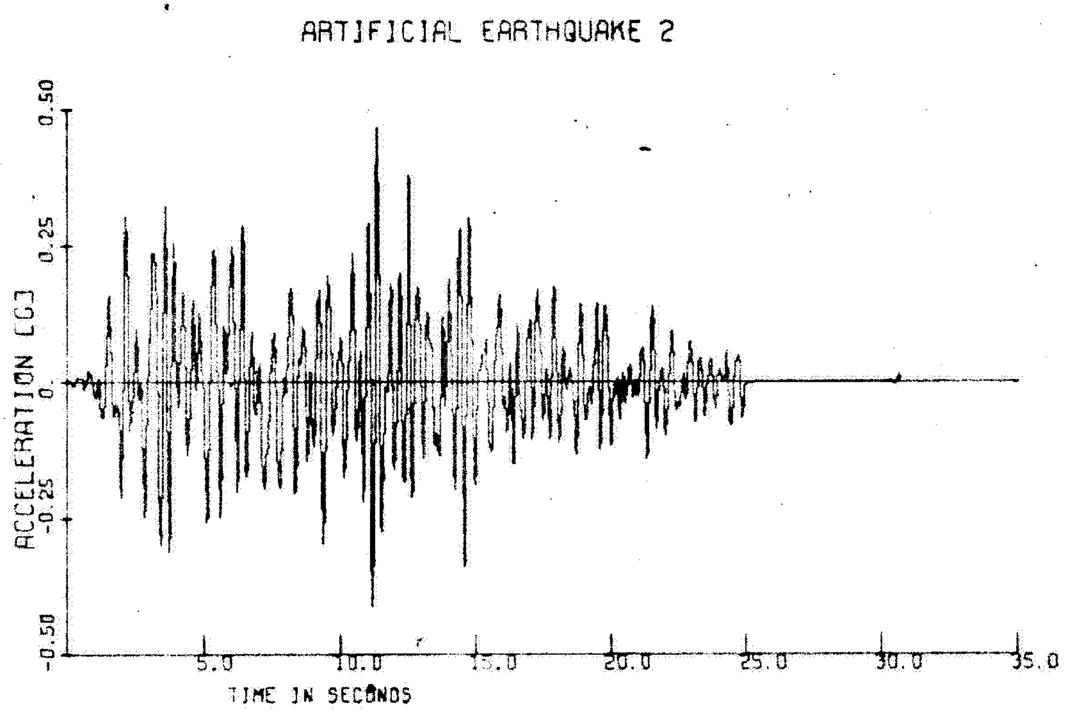

Time History of Surface Acceleration

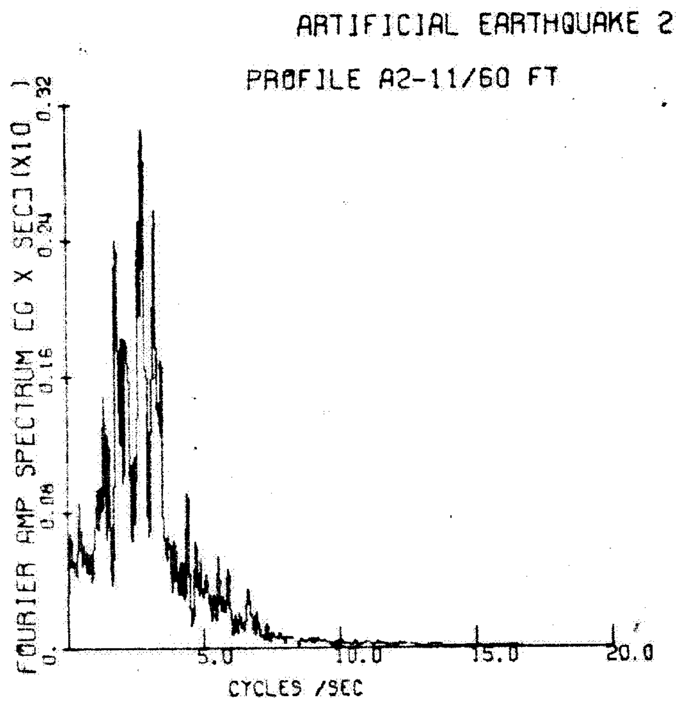

Fourier Amplitude Spectrum of Surface Motion

FIGURE 11. A6-9 (60 FT. TO BEDROCK)
SIMULATED EARTHQUAKE

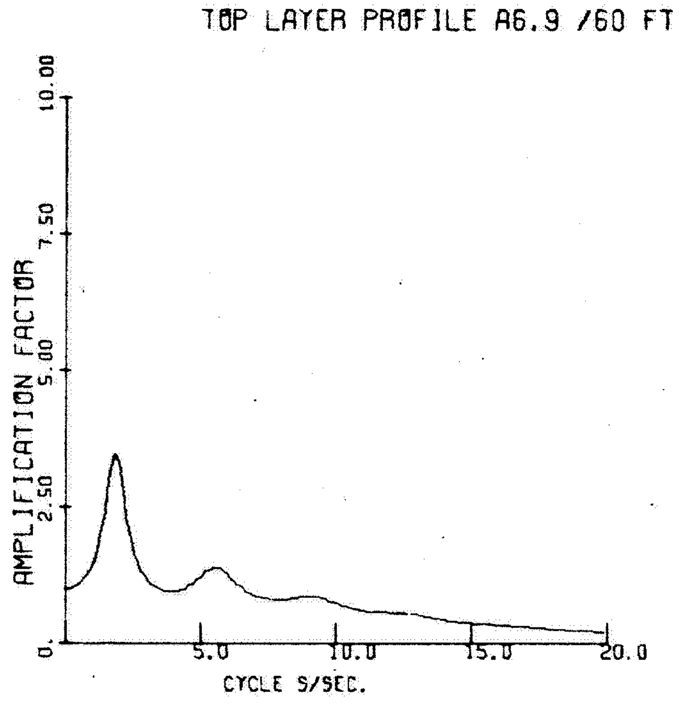

Soil Transfer Function

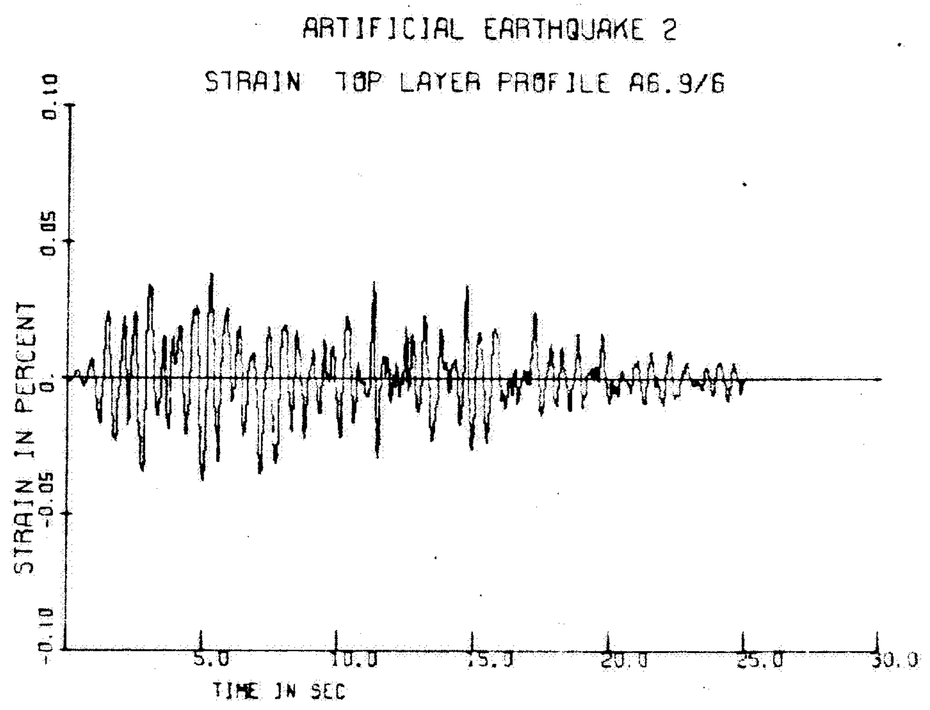

Time History of Strain on Top Soil Layer

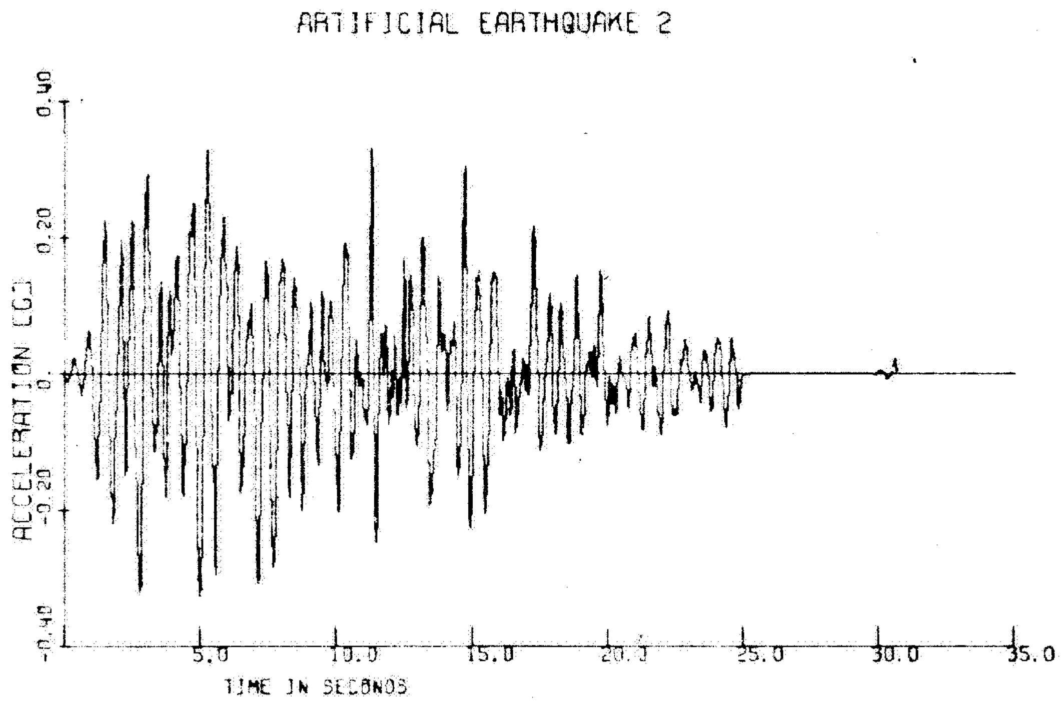

Time History of Surface Acceleration

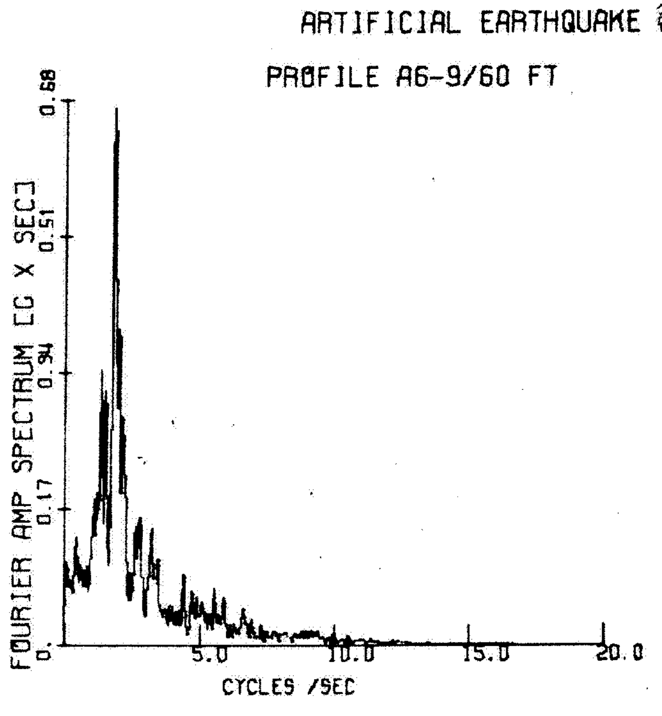

Fourier Amplitude Spectrum of Surface Motion

FIGURE 12. SOIL PROFILE A6-9 (200 FT. TO BEDROCK)
SIMULATED EARTHQUAKE

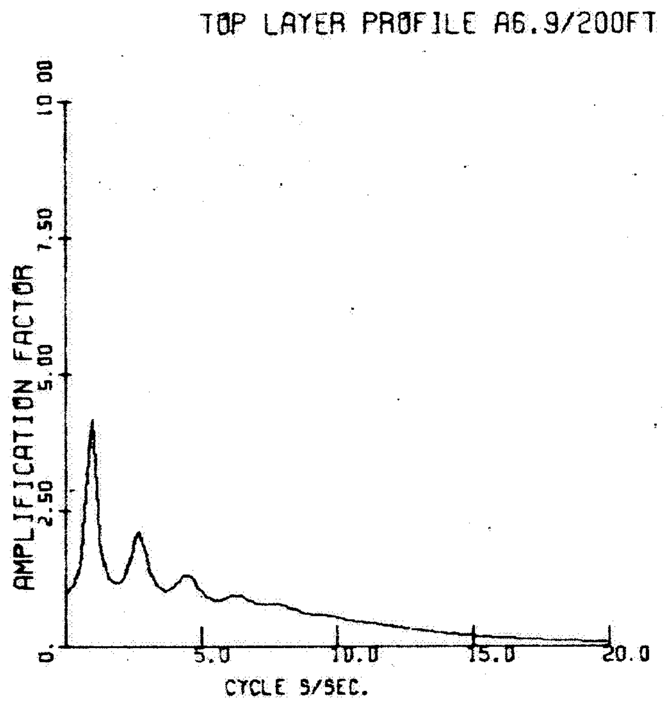

Soil Transfer Function

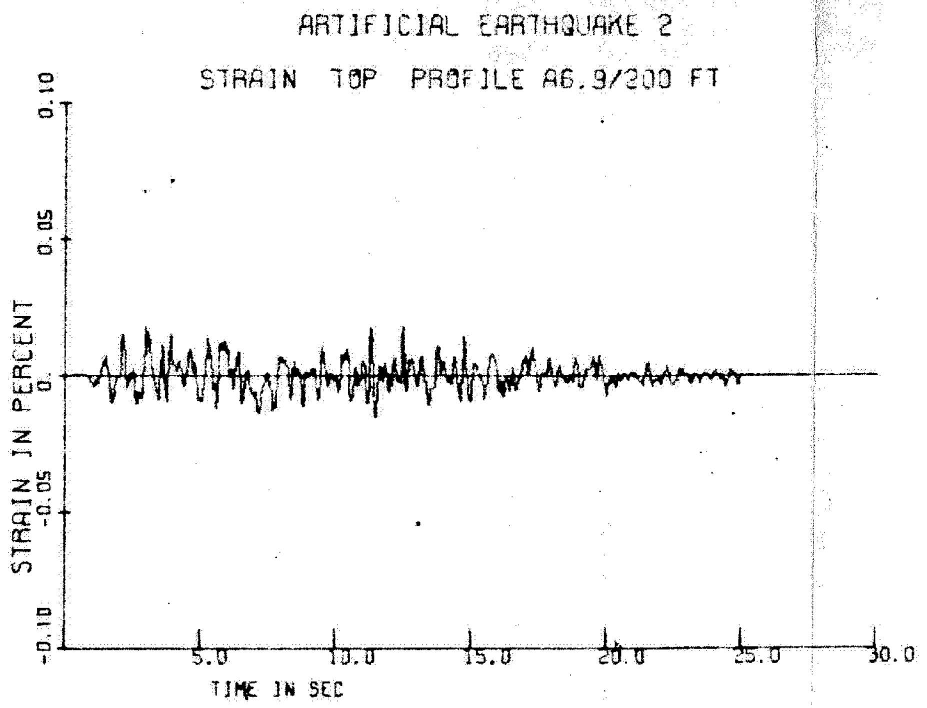

Time History of Strain in Top Soil Layer

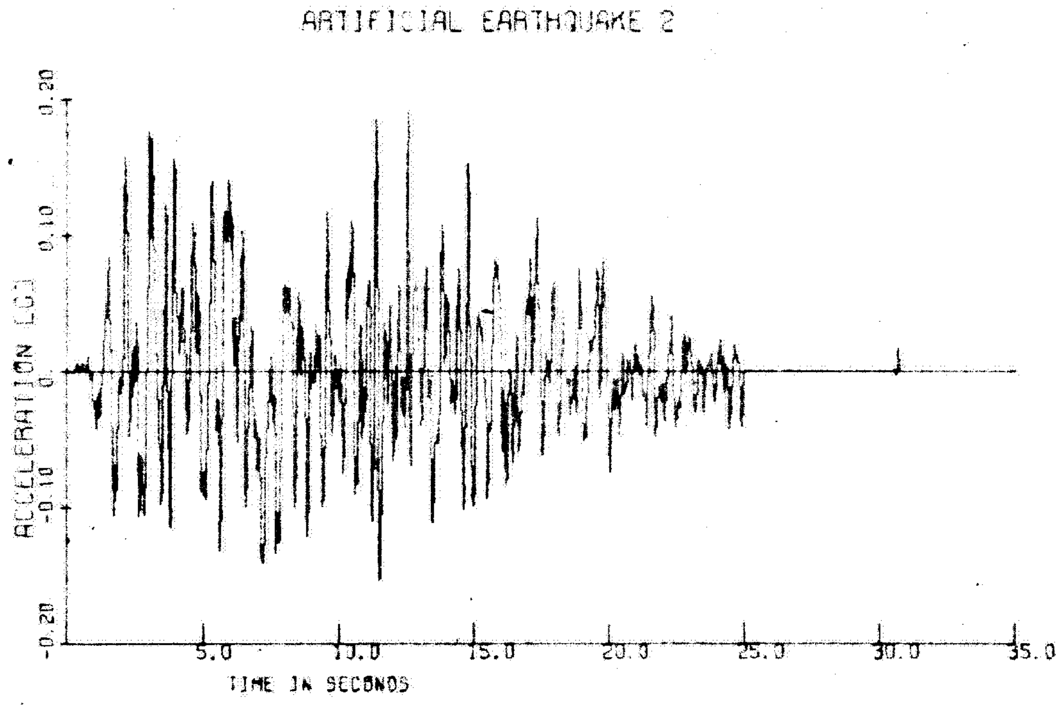

Time History of Surface Acceleration